

Characterization of Wafer-Level Au-In-Bonded Samples at Elevated Temperatures

THI-THUY LUU, NILS HOIVIK, KAIYING WANG, KNUT E. AASMUNDTVEIT,
and ASTRID-SOFIE B. VARDØY

Wafer-level bonding using Au-In solid liquid interdiffusion (SLID) bonding is a promising approach to enable low-temperature assembly and MEMS packaging/encapsulation. Due to the low-melting point of In, wafer-level bonding can be performed at considerably lower temperatures than Sn-based bonding; this work treats bonds performed at 453 K (180 °C). Following bonding, the die shear strength at elevated temperatures was investigated from room temperature to 573 K (300 °C), revealing excellent mechanical integrity at these temperatures well above the bonding temperature. For shear test temperatures from room temperature to 473 K (200 °C), the measured shear strength was stable at 30 MPa, whereas it *increased* to 40 MPa at shear test temperature of 573 K (300 °C). The fracture surfaces of Au-In-bonded samples revealed brittle fracture modes (at the original bond interface and at the adhesion layers) for shear test temperatures up to 473 K (200 °C), but ductile fracture mode for shear test temperature of 573 K (300 °C). The as-bonded samples have a layered structure consisting of the two intermetallic phases AuIn and γ' , as shown by cross section microscopy and predicted from the phase diagram. The change in behavior for the tests at 573 K (300 °C) is attributed to a solid-state phase transition occurring at 497 K (224 °C), where the phase diagram predicts a AuIn/ ψ structure and a phase boundary moving across the initial bond interface. The associated interdiffusion of Au and In will strengthen the initial bond interface and, as a consequence, the measured shear strength. This work provides experimental evidence for the high-temperature stability of wafer-level, low-temperature bonded, Au-In SLID bonds. The high bond strength obtained is limited by the strength at the initial bond interface and at the adhesion layers, showing that the Au-In SLID system itself is capable of even higher bond strength.

DOI: 10.1007/s11661-015-2865-9

© The Minerals, Metals & Materials Society and ASM International 2015

I. INTRODUCTION

SOLID liquid interdiffusion (SLID) wafer-level bonding is a promising technology for system integration that allows applications at temperatures higher than the actual bonding temperature. It enables the use of low-cost metallization, flux-free bonding, fine-pitch micro-interconnects, encapsulation, and probably the most important: repeated stacking/integration without re-melting the previously bonded materials.^[1] The bonding technique is based on the rapid formation of intermetallic compounds (IMCs) between two metal components, one being a low-melting and the second a high-melting component. The bonding temperature is usually kept above the melting point of the low-melting component. The layer thicknesses are designed such that the low-melting metal is completely consumed in the

process, leaving a final bond-line of IMCs with a higher re-melting temperature than the initial bonding temperature. Traditionally, the layer thicknesses are designed with excess high-melting point metal, resulting in remaining layers of this material after bonding.

For applications that require operation at, or exposure to, high temperatures the main requirements to the bonding material are that the bond-line has a high-melting point and that the shear strength remains high at elevated temperatures. In order to achieve high shear strength at elevated temperatures, it is important to minimize the thermally induced stresses in the bond stack; this is typically done by reducing the bonding temperature, having a low CTE mismatch between the utilized materials, and by having a good thermal conductivity. In this study, we have investigated the high-temperature integrity of Au-In SLID wafer-level bonded samples. Compared to the better known SLID systems Cu-Sn and Au-Sn which are assembled at 523 K to 573 K (250 °C to 300 °C) and 573 K to 623 K (300 °C to 350 °C),^[1-4] Au-In can be assembled using a lower bonding temperature 453 K (180 °C).^[5,6] This is of interest for many applications since a lower bonding temperature may reduce thermal stress in the package, and also facilitate bonding of temperature sensitive devices.^[7] Furthermore, with a properly designed

THI THUY LUU, PhD Candidate, NILS HOIVIK, KAIYING WANG, and KNUT E. AASMUNDTVEIT, Professors, are with the Department of Micro and Nanosystems technology (IMST), Buskerud and Vestfold University College, Raveien 215, 3184 Borre, Norway Contact e-mail: Thi.Luu@hbv.no ASTRID-SOFIE B. VARDØY, Research Scientist, is with the SINTEF ICT Instrumentation Department, Forskningsveien 1, 0373 Oslo, Norway.

Manuscript submitted June 13, 2014.

Article published online March 31, 2015

bond-line of Au-In, the final bond has demonstrated excellent reliability during thermal cycling and high-temperature storage/aging tests,^[5,6,8,9] as well as long-term hermeticity.^[10] Au-In wafer-level bonded samples have also shown bond-integrity up to 742 K (469 °C) by applying a load to a test specimen that was isothermally heated.^[11,12] Such tests, however, only determined the overall integrity, or re-melting temperature, and not the mechanical strength of the bonds at higher temperatures. With this study, we present for the first time the Au-In bond strength at elevated temperatures. The shear tests were conducted at different temperatures, from room temperature (RT) to 573 K (300 °C). Fractography of bonded and subsequently sheared samples was analyzed, using optical microscopy, scanning electron microscopy (SEM), energy dispersive X-ray spectroscopy (EDS), profilometry, and interferometry.

II. EXPERIMENTAL SETUP AND DESIGN OF TEST VEHICLES

For Au-In bonding, one of the major concerns is the rapid formation of IMCs, particularly AuIn₂, which is significant even at RT.^[13,14] By using the growth kinetics coefficient of AuIn₂ given by Zang *et al.*,^[13] the required time to consume In into AuIn₂ is estimated by

$$t = \frac{(tr_{\text{AuIn}_2/\text{In}} * y)^2}{k} \quad [1]$$

where t is the required time to consume all In into AuIn₂, y is the initial In thickness, $k = 1.55\text{E}-16 \text{ m}^2/\text{s}$ is the diffusion constant of AuIn₂ at room temperature which is extracted from Zang *et al.*,^[13] and $tr_{\text{AuIn}_2/\text{In}}$ refers to the thickness ratio of AuIn₂ and initial In. The ratio is estimated by

$$tr_{\text{AuIn}_2/\text{In}} = \frac{y_{\text{AuIn}_2}}{y_{\text{In}}} = \frac{m_{\text{AuIn}_2}/\rho_{\text{AuIn}_2}}{m_{\text{In}}/\rho_{\text{In}}} = \frac{1/10.27}{0.54/7.31} = 1.3 \quad [2]$$

Here m_{AuIn_2} is the total AuIn₂ mass, m_{In} is the In mass that is consumed into AuIn₂, 0.54 is the weight ratio of In in AuIn₂, ρ_{In} and ρ_{AuIn_2} are mass densities of In and AuIn₂, respectively.

Figure 1 illustrates the rapid formation of AuIn₂ at RT by showing the time required to convert all available In into AuIn₂ (assuming a sufficient amount of Au present) at RT by using Eq. [1]. From Figure 1, one can estimate that after RT storage for 24 hours, a 2.8- μm -thick layer of In would have been consumed. In a robust manufacturing process, one must allow the fabricated wafers to be stored for some time after deposition of In, and therefore the formation of AuIn₂ must be accounted for. To ensure there is pure In at the surface prior to bonding, the AuIn₂ growth should be limited by Au, and the required In/Au thickness ratio should be larger than the ratio corresponding to a complete conversion of all Au and In into AuIn₂, estimated to 3.1 by

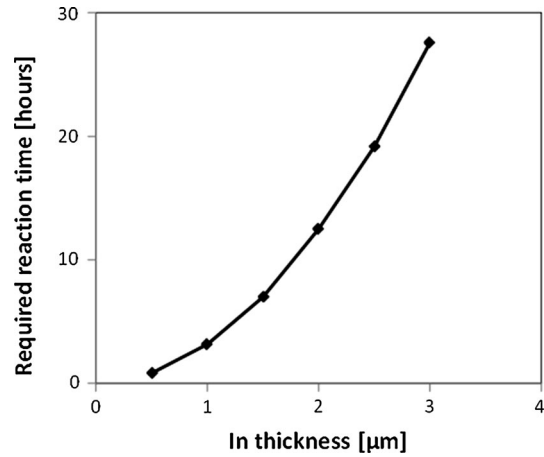


Fig. 1—Required time to consume all In into AuIn₂ at room temperature as function of In thickness, assuming Au surplus.

$$\frac{y_{\text{In}}}{y_{\text{Au}}} = \frac{m_{\text{In}}/\rho_{\text{In}}}{m_{\text{Au}}/\rho_{\text{Au}}} = \frac{0.54/7.31}{0.46/19.3} = 3.1. \quad [3]$$

Here m_{In} and m_{Au} are In and Au mass that are consumed into AuIn₂, 0.54 is the weight ratio of In in AuIn₂, 0.46 is the weight ratio of Au in AuIn₂, ρ_{Au} and ρ_{In} are mass densities of Au and In, respectively.

The design of test vehicles is shown in Figure 2. On each die and substrate there are two Au bond pads measuring $0.8 \times 1.0 \text{ mm}^2$. The In is evaporated using a lift-off process onto one of the wafers (which will form the top die) where the mask opening for each pad measures slightly less than the Au pad ($0.79 \times 0.99 \text{ mm}^2$) in order to compensate for the misalignment. Since the In and Au react and form AuIn₂ before the wafers are bonded, it is important that pure In exists on the surface prior to bonding. Therefore, we deposited 1.3 μm In onto 0.16 μm Au giving a In/Au ratio significantly larger than the requirement of 3.1. If all the Au reacts to form AuIn₂, the layer thickness will then be 0.7 μm AuIn₂ and 0.8 μm In. On the substrate wafer, the Au layer is intentionally thicker (0.8 μm) to ensure ample amount of Au to react with In. The final bond-line should comprise Au and/or Au-In IMCs without any unreacted In remaining. This approach has allowed us to obtain Au-In wafer-level bonding with 100 pct yield using wafers stored at RT for 1 month.

With the thicknesses given above, the overall estimated mole fraction of In will be

$$\begin{aligned} \frac{n_{\text{In}}}{n_{\text{Au}}} &= \frac{y_{\text{In}} \rho_{\text{In}} M_{\text{Au}}}{y_{\text{Au}} \rho_{\text{Au}} M_{\text{In}}} = 0.65 \frac{y_{\text{In}}}{y_{\text{Au}}} \\ &= 0.85 \rightarrow \frac{n_{\text{In}}}{n_{\text{In}} + n_{\text{Au}}} = 0.46. \end{aligned} \quad [4]$$

Using the Au-In equilibrium phase diagram shown in Figure 3 and an In mole fraction of 0.46, we can expect that the final intermetallic phases present in the

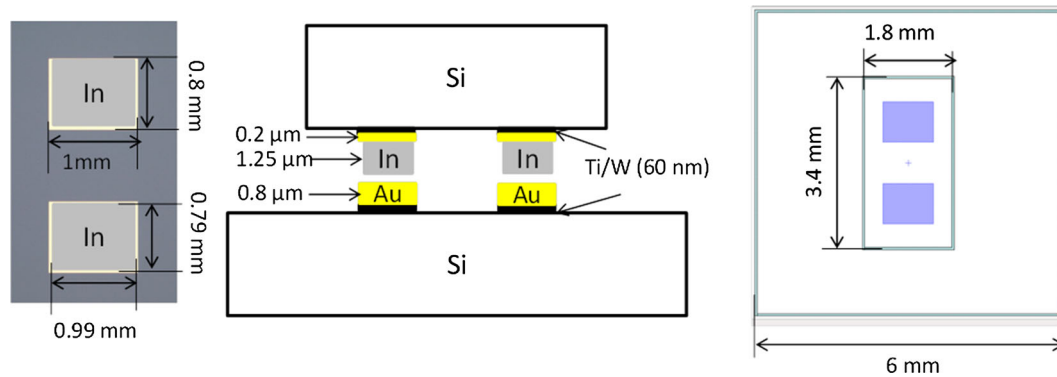


Fig. 2—Design of bond structure. Chip size is $1.8 \times 3.4 \text{ mm}^2$. Substrate size is $6 \times 6 \text{ mm}^2$. The dimensions of Au pads are $0.8 \times 1 \text{ mm}^2$. The dimension of deposited In on Au pads is $0.79 \times 0.99 \text{ mm}^2$. The Ti-W layer thickness is 60 nm. For the die side, Au/In thickness is $0.2 \text{ μm}/1.3 \text{ μm}$. For the substrate side, Au thickness is 0.8 μm .

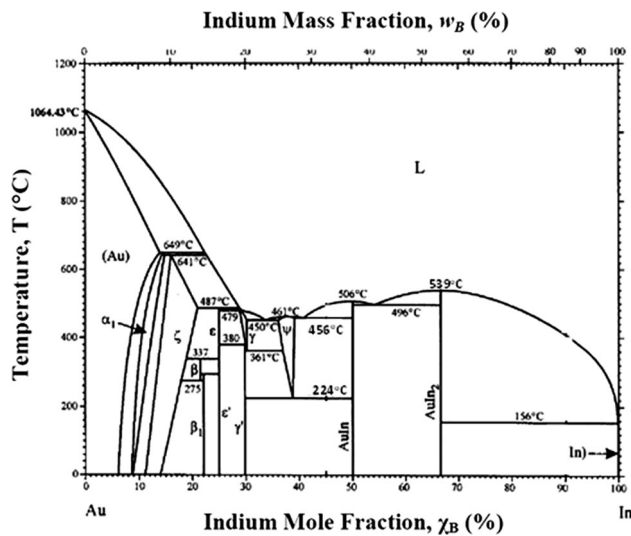


Fig. 3—Au/In-phase diagram. For In mole fraction of 0.46, the expected final bond-line is AuIn and γ' phases.

bond-line will be a mixture of AuIn and γ' if thermal equilibrium is reached. Previously, Grummel *et al.*^[5] demonstrated that, with In mole fraction lower than 0.67, Au-In bonding promised excellent reliability after thermal cycling tests. Based on the In mole fraction and the given thicknesses of Au and In, the estimated final phase thicknesses correspond to 1.7 μm AuIn and 0.5 μm γ' -phase.

For all wafer-bonding experiments, we used 4-inch Si wafers with a 100-nm-thick thermally grown SiO_2 layer, a 60-nm-thick Ti-W adhesion layer, and a 0.16/0.8- μm -thick sputtered Au layer. The Au layer was etched by ($\text{KI} + \text{I}_2$), and Ti-W was etched using H_2O_2 . The 1.3- μm -thick In layer was evaporated onto the die wafer, using thermal evaporation. Photoresist AZ4562 defined the In pads, and lifted off using acetone at 353 K (80 °C). The wafers were aligned on an EVG 620 mask-bond aligner and bonded at 453 K (180 °C) for 30 minutes, using an EVG 501 wafer-bonder. Due to the excess thickness of deposited In on the thin Au layer, the rapid formation of IMCs between In and Au did not prevent successful

bonding even for wafers stored approximately 24 hours between In evaporation and wafer bonding.

The bonded wafers were further diced into separate chips, as shown in Figure 2, with die dimensions of $1.8 \times 3.4 \text{ mm}^2$ and substrate dimensions of $6 \times 6 \text{ mm}^2$ to fit the specialized die-holder on the shear tester. The bonded samples were later cross-sectioned and further polished using ion milling before optical microscopy and SEM investigation. EDS was used to determine the elemental composition in the bond-line.

The samples were die shear tested using a NordsonDage 4000Plus shear-tester with the substrate placed on a built-in hotplate, using a 200-kgf load carriage. The test height was 75 μm above the substrate, and a test speed of 10 μm/s was used. Detail of shear test configuration is shown in Figure 4. At each shear test temperature; RT, 373 K, 473 K, and 573 K (100 °C , 200 °C , and 300 °C); between six and eight samples were tested. A custom made substrate holder^[15] was used in order to align and prevent rotation of the samples during testing. Lastly, fractography of all the sheared surfaces was investigated using optical microscopy, SEM, EDS, profilometry, and interferometry.

III. RESULTS

After bonding, the dicing yield (the percentage of dies that remains after dicing) is a good indication of the strength of the bonded surfaces. For our wafers, we observed 100 pct yield. Cross section microscopy of the bond-lines after ion milling shows two distinct intermetallic phases, as seen in Figure 5. The Au/In atomic ratio is measured by EDS analysis to be 50/50 (in the top layer) and 70/30 (in the bottom layer). Although layer thicknesses are small compared to the lateral resolution of EDS ($\sim 2 \text{ μm}$ at an acceleration voltage of 15 kV), it is still natural to assign these phases as AuIn-phase and γ' -phase, respectively. The measured thicknesses of these two phases (1.7 μm for the AuIn and 0.6 μm for the γ' -phase) match the values estimated from original Au and In layer thicknesses (1.7 μm AuIn and 0.5 μm γ' -phase) well.

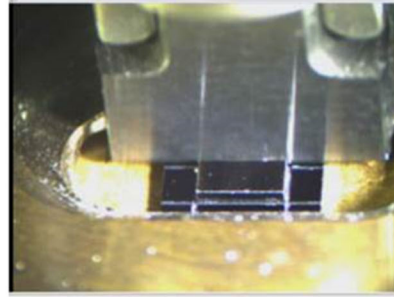
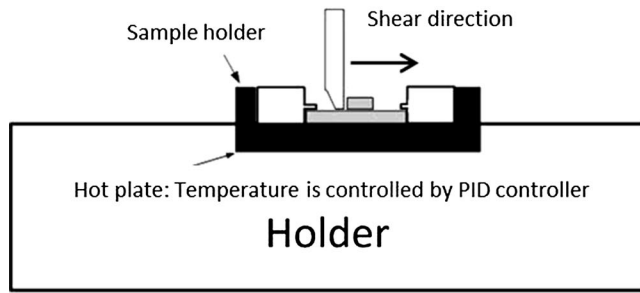


Fig. 4—Illustration of shear test configuration. The bonded sample is attached and clamped to the hot plate, using a custom sample holder. The holder is designed to efficiently transfer heat from the hot plate to the test sample. A PID controller controls the temperature of the hot plate. The entire temperature range was calibrated to ensure that the actual measured temperature on hot plate matches the indicated temperature on PID controller.

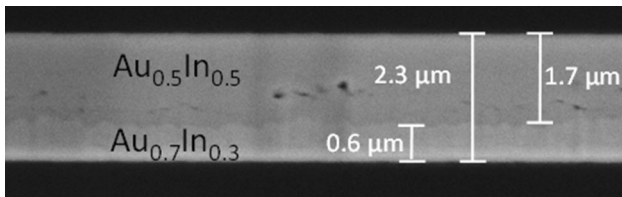


Fig. 5—SEM cross section image of bonded sample at 2800 times magnification. Two Au-In intermetallic compounds (IMCs) are present in the final bond-line, with In mole fraction 50 and 30 pct, respectively, interpreted as the AuIn and γ' phases. The total intermetallic thickness is $2.3 \mu\text{m}$. The thickness matches the estimation based on initial Au and In thicknesses: $1.7 \mu\text{m}$ AuIn/ $0.5 \mu\text{m}$ γ' .

The measured die shear strength at different shear test temperatures is shown in Figure 6. From RT to 473 K (200 °C), the shear strength is stable at 30 MPa, whereas at 573 K (300 °C) the shear strength increases significantly to 40 MPa. This confirms that the presented Au-In bonding results in a solid bond-line with high bond strength up to 573 K (300 °C).

With a final bond-line with two phases present, as shown in Figure 5, there are several possible fracture regions. An adhesive fracture may occur at the Ti-W adhesion layer (observed to always happen at the Ti-W to intermetallic interface), or between the two phases in the bond line. We therefore denote adhesive failures between Ti-W and AuIn as (a), between Ti-W and γ' -phase as (e) and between the two phases as (c). Any cohesive fracture will take place inside the AuIn layer (b) or γ' -layer (d). Figure 7 illustrates these regions and corresponding fracture modes.

Figure 8 shows a typical fracture surface of a test sample at RT, as measured by SEM/EDS and with interferometry. We observe three different, very well-defined, fracture surfaces: adhesive fracture at the die side between Ti-W and AuIn layer (a), adhesive fracture at the substrate side between Ti-W and γ' -layer (e), and fracture inside the AuIn layer (b). EDS measurements shown in Figure 8(a) give the average over a probing depth of $\sim 0.4 \mu\text{m}$ (at an acceleration voltage of 15 kV), and can thus have contributions from more than one phase. The height profile in Figures 8(b) and (c) shows that the different fracture surfaces are planar, including the fracture inside the AuIn layer. The position of this

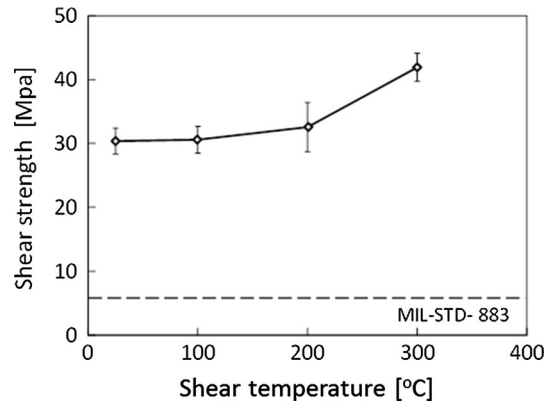


Fig. 6—Shear strength as function of shear test temperature. At each temperature, six to eight samples were tested. The shear strength is stable at 30 MPa from RT to 473 K (200 °C). At 573 K (300 °C), the shear strength increases to 40 MPa. At 473 K (200 °C), there is more variation of shear strength due to fracture in Si die side.

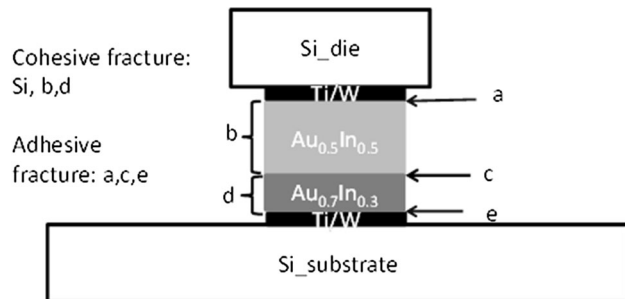


Fig. 7—Schematic of cross section and possible failure positions of bonded samples. There are five possible fracture positions: adhesive fracture between AuIn and Ti-W layers (a), cohesive fracture inside AuIn layer (b), adhesive fracture between AuIn and γ' layers (c), cohesive fracture inside γ' layer (d), and adhesive fracture between γ' and Ti-W layers (e).

fracture corresponds to the initial bond interface between the substrate and the die, indicating that this initial interface is a weak link in the system. All height measurements from interferometry were confirmed by profilometry. The area of different fracture surfaces were deducted from interferometry data. Similar fractographies were recorded for all the tested samples sheared at

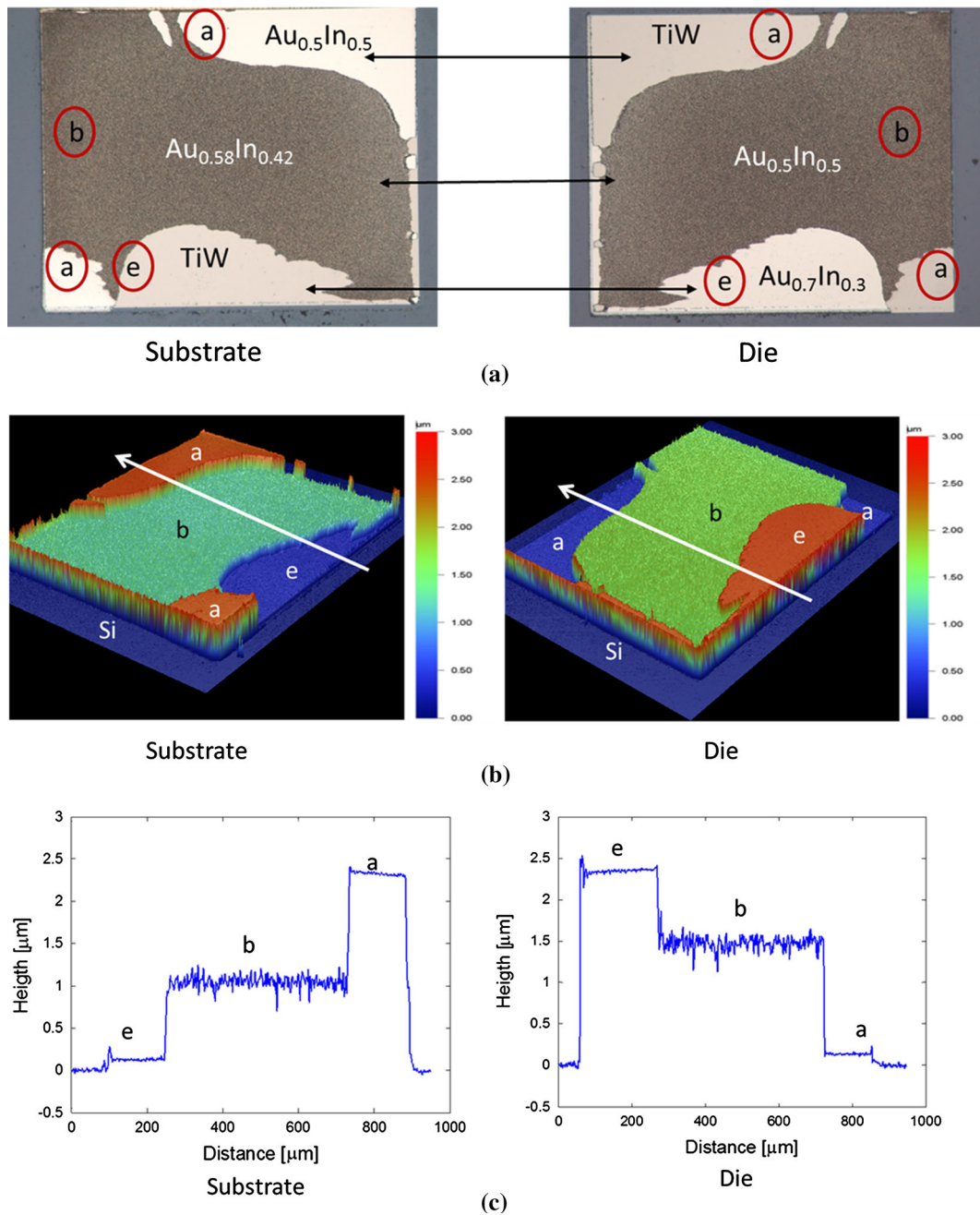


Fig. 8—Typical fracture mode for shear testing at RT. Three different fracture positions were observed: adhesive fracture between Ti-W and AuIn layers (a), cohesive fracture inside AuIn layer (b), and adhesive fracture between Ti-W and γ' layers. The height profile shows that the fracture surface is planar, and the fracture has a brittle failure mode. (a) Microscope picture of fracture surface and surface EDS analysis result. (b) 3D fracture height profile taken by interferometer. (c) Height profile measurement across tested sample surface.

RT, 373 K and 473 K (100 °C and 200 °C). For these samples, a majority of the fracture surfaces reveal a brittle failure mode. It is noteworthy to point out that at 473 K (200 °C), we observed that the Si die shattered for several tested samples. One example of this is shown in Figure 9 where a remaining piece of the Si die can be seen.

Figure 10 shows the surface of a sample shear tested at 573 K (300 °C), with a fundamentally different fracture mode from what is observed for lower shear

temperatures. There are no distinctly planar fracture surfaces, clearly showing a more ductile failure mode. Two different fracture regions dominate: adhesive fracture at the die side between Ti-W and AuIn layer (a), and fracture inside the intermetallic layers (corresponding to the b/c/d positions in Figure 7).

Table I lists the average percentage area for the various fracture surfaces at the respective failure modes. Due to substantial sample-to-sample variation, there is a noticeable difference between these average values and

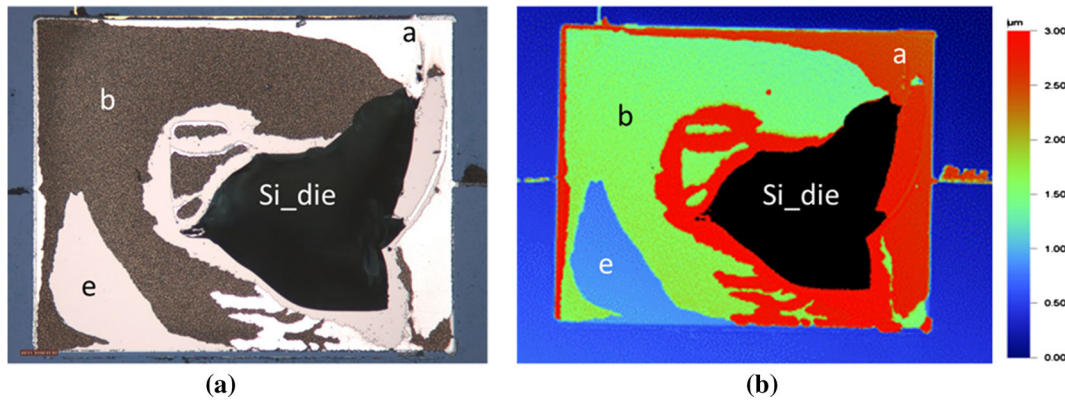


Fig. 9—Particular fracture surface at substrate side for sample shear tested at 473 K (200 °C). Four fracture positions were observed: cohesive fracture at Si die and in AuIn layer (b), and adhesive fracture at Ti-W layer (a, e). (a) Microscope picture. (b) 2D height profile.

the single-sample values that are deduced from Figures 8 through 10. From RT to 473 K (200 °C), the areas of different fracture surfaces are similar. At 573 K (300 °C), there is a change of fracture modes, with a much less precisely defined fracture surface.

IV. DISCUSSION

Our measurements show Au-In SLID bonding with high mechanical integrity, with die shear strength much higher than the minimum requirement given by MIL-STD-883 of 6 MPa. The initial layer thicknesses of Au and In are designed with excess In on the Au-In wafer, in order to allow Au-In interdiffusion during storing of samples prior to bonding. With this thickness ratio design, we believe the wafers could be stored longer at RT prior to bonding. This has been verified in a separate experiment, where a successful bonding with 100 pct dicing yield was obtained with the wafers that were stored at RT for one month prior to bonding. At the time of bonding, the metallization of this wafer will consist of pure In and IMCs, with all the Au reacted. This is opposed to the common SLID process used for Cu-Sn or Au-Sn,^[1] where a remaining layer of the ductile, high-temperature stable metal is desired. For Au-In, this would not be compatible with manufacturability, due to the rapid interdiffusion of Au-In, easily jeopardizing the possibility of having remaining In for bonding, if the initial layer thicknesses are designed with excess Au. Whereas Cu-Sn and Au-Sn SLID bonds typically are composed of an intermetallic compound (IMC) layer sandwiched between layers of pure Cu (or Au); the Au-In SLID bonds in this work are composed entirely of IMCs.

According to our measurements, the die shear strength does not change significantly for shear test temperatures from RT to 473 K (200 °C), also above the melting temperature of In at 429 K (156 °C). This is as predicted, since no pure In is expected to remain in the bond-line, and all Au-In IMCs have melting points above 723 K (450 °C), according to the phase diagram (Figure 3). The die shear strength increases significantly

at 573 K (300 °C). The re-melting temperature of Au-In-bonded samples has previously been shown to exceed 742 K (469 °C).^[11] The similarity in fracture mode for samples tested between RT and 473 K (200 °C) furthermore indicates that there is no significant change in the microstructure and mechanical properties of the phases present. The observed increase in standard deviation for the samples tested at 473 K (200 °C) we believe can be explained by the shattering of the top Si die during shear testing. The exact reason why this shattering mostly occurred at 473 K (200 °C) is not known, but most probably it is caused by a small rotation of the die-holder caused by the increase in temperature on the test stage, and not from the sample itself.

From height measurements of the fracture surface for dies tested from RT to 473 K (200 °C), we observe three different failure modes: adhesive fractures at the Ti-W to AuIn and Ti-W to γ' interfaces (a and e), and fracture inside the AuIn layer (b), occurring at the position of the initial bond interface. The limiting factors for the strength are thus observed to be the adhesion layers and the initial surfaces of the metallization on the substrate and chip. If an application should require an even higher strength than our observations, this would call for a closer investigation of the adhesion layer to intermetallic interface, as well as the cleanliness and the oxidation state of the initial surfaces.

At a shear test temperature of 573 K (300 °C), we observe an increase in shear strength, as well as a change in the fracture mode. Based on height measurement of the fractured surfaces, as shown in Figure 10, the fracture appears to have been in the middle region of the bond-line. But opposed to the shear tests at 473 K (200 °C) and lower temperatures, the fracture does not follow a well-defined surface and cannot be directly related to the original bond interface. The Au and In mole fraction from EDS analysis shows an elemental composition of Au_{0.59}In_{0.41} (substrate) and Au_{0.56}In_{0.44} (die) as seen from the fracture surface. The phase diagram (Figure 3) shows a potential phase transition to the ψ -phase at temperatures above 497 K (224 °C), as this phase having an In mole fraction of 0.37 to 0.39 at 573 K (300 °C). This is close to the elemental compo-

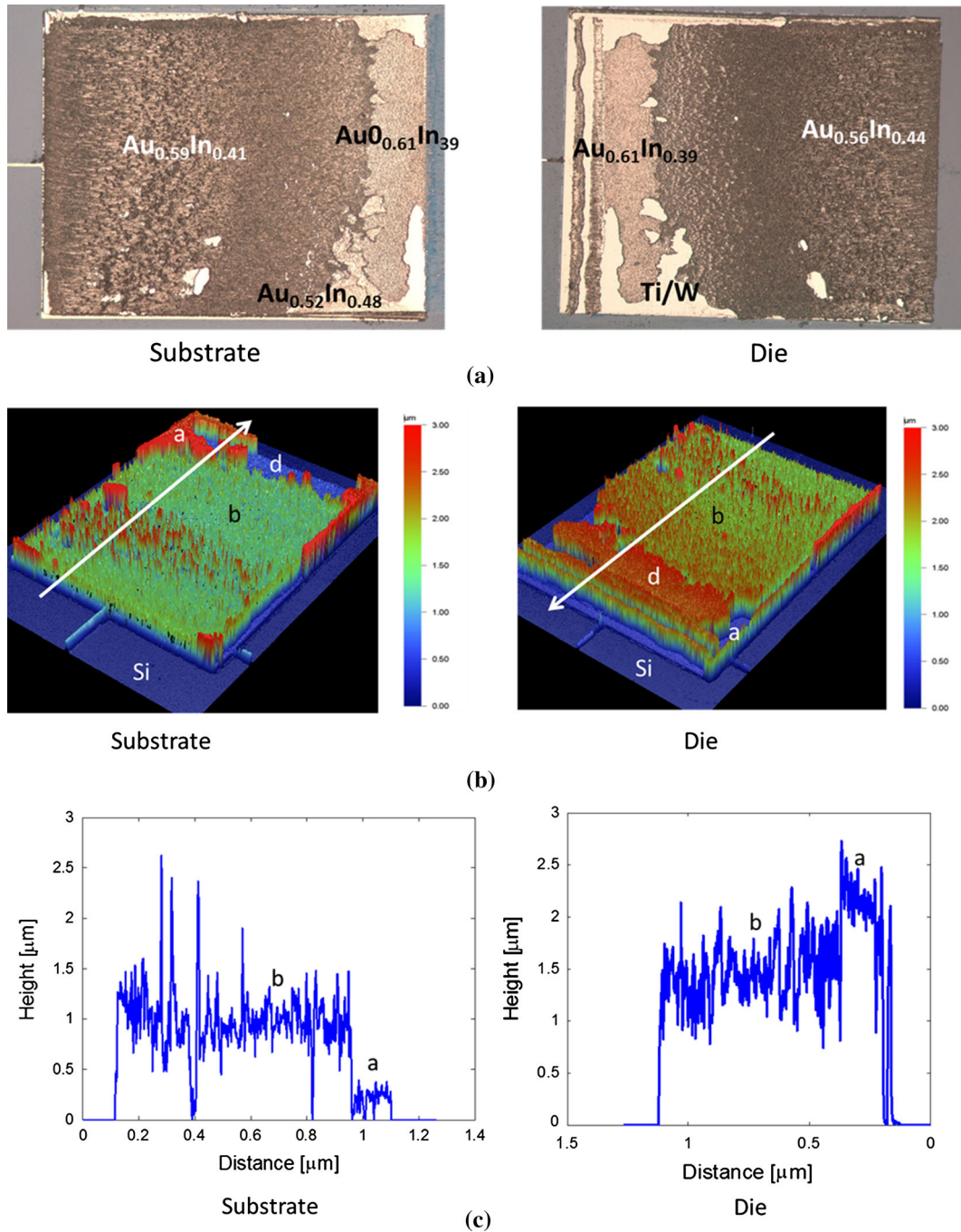


Fig. 10—Typical fracture mode for sample shear tested at 573 K (300 °C). The surface presents a ductile failure mode. The fracture surface is not planar. EDS analysis indicates the presence of ψ phase. (a) Microscope picture of fracture surface and surface EDS analysis result. (b) 3D fracture height profile taken by interferometer. (c) Height profile measurement across tested sample surface.

sition observed in the fracture surfaces (note that the EDS data at the die side is expected to include contributions from the AuIn phase), so we can conclude that such a phase transition has taken place.

Assuming thermal equilibrium at 573 K (300 °C), our overall In mole fraction of 0.46 will result in ψ -phase (at the substrate side) and AuIn phase (at the die side). This is in accordance with the observed EDS values. The initial Au and In thicknesses correspond to thicknesses of 1.0 μm ψ -phase and 1.3 μm AuIn. Basing the

calculations on the observed thicknesses in the as-bonded sample (Figure 5) gives closely similar values: 1.1 μm ψ -phase and 1.2 μm AuIn.

For the as-bonded sample, the original bond interface lies within the AuIn phase (comparing Figures 2 and 5). EDS data from the fracture at the original bond interface (Figure 8) support this: AuIn is found at the die side, whereas the substrate side has a lower In content consistent with data from both AuIn and γ' . The layer thicknesses are of the same order as the EDS

Table I. Average Area Fraction at Different Places of Shear Test Samples

Shear Test Temperature	Si (Die)	a (Ti-W Die)	b (Initial Bond Interface Inside AuIn ₂)	c AuIn/ γ' Interface)	d (Inside γ' Layer)	e (Ti-W Substrate)
RT	0	36	51	0	0	13
373 K (100 °C)	0	37	48	0	0	15
473 K (200 °C)	6	39	40	0	0	15
573 K (300 °C)*	0	54	38			8

*The different fracture modes, as well as the phase transitions expected at 497 K (224 °C), make the classification into b/c/d not applicable.

measurement depth, so the surface layer cannot be distinguished from the underlying one. For thermal equilibrium at 573 K (300 °C) as described above, the original bond interface lies within the ψ -phase. At the phase transition [497 K (224 °C)], the interface between the different IMCs will move toward the die side as the ψ -phase grows, moving across the original bond interface. The interdiffusion of Au and In needed for this to happen explains the strengthening at the original bond interface so this no longer is the site of fracture. This is reflected both in the absence of a planar, brittle fracture, as well as in the higher shear strength observed at 573 K (300 °C).

Table I indicates a slight increase in the relative amount of fracture at the adhesion layers at 573 K (300 °C), particularly at the die (AuIn) side. This is a direct effect of the strengthening of the bond described above, assuming that the interface between the adhesion layers and the IMCs is not significantly changed by the temperature change from 473 K to 573 K (200 °C to 300 °C). The relative amount of fracture at the adhesion layer at the substrate (ψ -phase) is quite low, indicating that this particular phase has acceptable adhesion to the Ti-W layer.

For all sheared samples from RT to 573 K (300 °C), a high fraction of adhesive fracture between Ti-W and IMCs was observed. This implies that the bonded layer is stronger than the adhesion layer. This is different from our observation for Cu-Sn SLID bonding,^[16] using a similar adhesion layer, where less fracture tends to occur at the Ti-W to Au seed layer interface. As noted above, Cu-Sn SLID bonding is typically designed with excess Cu, whereas our Au-In is not designed with excess Au. The excess Cu layer isolates the IMCs layers from the adhesion layer and prevents Sn from interacting with it. For our Au-In bonding, the interface to the adhesion layer changes during bonding: the adhesion layer to Au interface becomes an adhesion layer to IMC interface after bonding. We assume that this also influences the adhesion strength. Thus, the adhesion layer becomes a limiting factor in our Au-In SLID bonding, but not in our Cu-Sn SLID bonding. We emphasize that the actual strength of our Au-In bonds is indeed very high.

V. CONCLUSIONS

Au-In SLID wafer-level bonding at 453 K (180 °C), with a proper design of the metal thicknesses for Au and In, results in a very high bonding yield and a high

resulting shear strength: in the 30 MPa range. The shear strength is constant when the shear test temperature is increased from room temperature to 473 K (200 °C), and *increases* to ~40 MPa when the shear test temperature is increased to 573 K (300 °C). This verifies experimentally that Au-In SLID bonding, performed at temperatures right above the melting temperature of In 429 K (156 °C), is indeed very suitable for high-temperature applications. Phase diagram predictions call for stability to 723 K (450 °C), and we demonstrate high strength up to our highest testing temperature of 573 K (300 °C).

The bond-line consists of the intermetallic phases AuIn and γ' , as found by cross section microscopy and EDS. Interferometry of the fractured, sheared samples reveals that at temperatures up to 473 K (200 °C), the samples fracture at the well-defined planar surfaces: either at the adhesion layer to intermetallic interfaces, or at the position of the original bond interface. At 573 K (300 °C), the nature of the fracture changes to a ductile fracture, explained by a phase transition to the ψ -phase and an annealing effect as the IMC-to-IMC phase boundary sweeps across the original bond interface. The higher overall bond strength at 573 K (300 °C) results from this improved strength of the initial bond interface.

ACKNOWLEDGMENTS

We would like to acknowledge to the e-Brains Project FP7-ICT-257488 and Oslofjordfondet Project 208929 for the funding, and the lab engineers Zekija Ramic, Ragnar Dal Johansen at the Department of Micro and Nanosystems Technology, Buskerud and Vestfold University (IMST-HBV) for the laboratory support.

REFERENCES

1. N. Hoivik and K. Aasmundtveit: *Wafer-Level Solid-Liquid Interdiffusion Bonding, Handbook of Wafer Bonding*, Wiley-VCH Verlag GmbH & Co. KGaA, Weinheim, 2012, pp. 181–214.
2. H. Xu, T. Suni, V. Vuorinen, J. Li, H. Heikkinen, P. Monnoyer, and M. Paulasto-Kröckel: *Adv. Manuf.*, 2013, vol. 1, pp. 226–35.
3. S. Giudice and C. Bosshard: *Microelectronics Packaging Conference (EMPC), 2013 European*, 2013, pp. 1–5.
4. A. Lapadatu, T.I. Simonsen, G. Kittilsland, B. Stark, N. Hoivik, V. Dalsrud, and G. Salomonsen: *ECS Trans.*, 2010, vol. 33, pp. 73–82.
5. B. Grummel, H.A. Mustain, Z.J. Shen, and A.R. Hefner: *2011 IEEE 23rd International Symposium on Power Semiconductor Devices and ICs (ISPSD)*, 2011, pp. 260–63.

6. C. Won Kyoung, C.S. Premachandran, C. Ong Siong, L. Xie, E. Liao, A. Khairyanto, B. Ratmin, K.C.W. Sheng, T. Phyo Phyo, and J.H. Lau: *59th Electronic Components and Technology Conference, 2009. ECTC 2009*, 2009, pp. 333–38.
7. W. Qian, J. Kyudong, C. Minseog, K. Woonbae, H. Sukjin, J. Byunggil, and M. Changyoul: *7th International Conference on Electronic Packaging Technology, 2006. ICEPT '06*, 2006, pp. 1–5.
8. T.B. Wang, Z.Z. Shen, R.Q. Ye, X.M. Xie, F. Stubhan, and J. Freytag: *J. Electron. Mater.*, 2000, vol. 29, pp. 443–47.
9. L. Chien-Chih, L. Yen-Kuang, H. Mau-Phon, and W. Yeong-Her: *IEEE Trans. Compon. Packag. Technol.*, 2003, vol. 26, pp. 635–41.
10. W.C. Welch and K. Najafi: *IEEE 21st International Conference on Micro Electro Mechanical Systems, 2008. MEMS 08*, 2008, pp. 806–09.
11. S. Yoon-Chul, W. Qian, H. Suk-Jin, J. Byung-Gil, J. Kyu-Dong, C. Min-Seog, K. Woon-Bae, and M. Chang-Youl: *57th Proceedings Electronic Components and Technology Conference, 2007, ECTC '07*, 2007, pp. 633–37.
12. C.C. Lee, C.Y. Wang, and G. Matijasevic: *IEEE Trans. Compon. Hybrids Manuf. Technol.*, 1993, vol. 16, pp. 311–16.
13. W. Zhang and W. Ruythooren: *J. Electron. Mater.*, 2008, vol. 37, pp. 1095–101.
14. Y.M. Liu and T.H. Chuang: *J. Electron. Mater.*, 2000, vol. 29, pp. 405–10.
15. T. Tollefsen, O. Løvvik, K. Aasmundtveit, and A. Larsson: *Metall. Mater. Trans. A*, 2013, vol. 44A, pp. 2914–16.
16. A. Campos-Zatarain, D. Flynn, K. Aasmundtveit, N. Hoivik, K. Wang, T.-T. Luu, M. Mirgizoudi, and R.W. Kay: *Design, Test Integration and Packaging (DTIP)*, 2014.